Bifacial PV cell with reflector for stand-alone mast for sensor powering purposes

Jakobsen, Michael Linde; Thorsteinsson, Sune; Poulsen, Peter Behrensdorff; Riedel, Nicholas; Rødder, Peter M.; Rødder, Kristin

Published in:
AIP Conference Proceedings

Link to article, DOI:
10.1063/1.5001437

Publication date:
2017

Document Version
Publisher's PDF, also known as Version of record

Bifacial PV cell with reflector for stand-alone mast for sensor powering purposes

Michael L. Jakobsen, Sune Thorsteinsson, Peter B. Poulsen, N. Riedel, Peter M. Rødder, and Kristin Rødder

Citation: AIP Conference Proceedings **1881**, 070004 (2017); doi: 10.1063/1.5001437
View online: http://dx.doi.org/10.1063/1.5001437
View Table of Contents: http://aip.scitation.org/toc/apc/1881/1
Published by the American Institute of Physics

Bifacial PV Cell with Reflector for Stand-alone Mast for Sensor Powering Purposes

Michael L. Jakobsen[1, c)], Sune Thorsteinsson[1, b)], Peter B. Poulsen[1, a)], N. Riedel[1], Peter M. Rødder[2] and Kristin Rødder[2]

[1] *Department of Photonics Engineering, Technical University of Denmark, mlja@fotonik.dtu.dk, Roskilde, Denmark.*
[2] *SolarLab, pmr@solarlab.dk, Viby J., Denmark.*

[a)]Corresponding author: ppou@fotonik.dtu.dk
[b)]sunth@fotonik.dtu.dk
[c)]mlja@fotonik.dtu.dk

Abstract. Reflectors to bifacial PV-cells are simulated and prototyped in this work. The aim is to optimize the reflector to specific latitudes, and particularly northern latitudes. Specifically, by using minimum semiconductor area the reflector must be able to deliver the electrical power required at the condition of minimum solar travel above the horizon, worst weather condition etc. We will test a bifacial PV-module with a retroreflector, and compare the output with simulations combined with local solar data.

INTRODUCTION

Bifacial solar modules are commercially attractive, due to the fact that the total energy producing area increases by a factor of two, and only to an additional module cost of approximately 30 %.[1] However, the challenge is to guide light onto both sides sufficiently efficient. Several works have proven that adding reflectors to bifacial panels mounted at a certain optimized tilt, increases the energy harvest even further, [2-3] and bifacial panels has offered new solutions as e.g. PV based fences.[4] For PV-systems mounted at a tilt, the reflectors will in many cases be placed underneath the PV panel to reflect incident light from surroundings e.g. the albedo. Since these reflectors are not exposed to rain they do not have the same self-cleaning ability as the PV panels itself and the resulting energy harvest is decreased due to soiling.[2, 4]

Earlier, we have proposed a system, using a vertical mounted bifacial panel and two vertical reflectors[5] mounted at an angle to partly reduce the soiling problem, but also to optimize the energy harvest. The schematics is illustrated in figure 1. The investigation of this system has been based on raytracing with different assumptions to simplify the model. One of the assumptions is that the irradiance of sunlight incident onto a surface, being normal to the sun all day, is constant.

The conclusions on the following investigations were that the bifacial PV-cell, combined with a retroreflector, including a transparent filling material, could collect 96 % of all light, incident onto a plane surface with the same area as both sides of the bifacial PV-cell together.[6] With and without the filling the simulated amount of incident light is plotted in figure 2 as a function of azimuth angular position of the sun.

In this work, we will include experimental solar data to estimate a more realistic incidence of sunlight in our simulations to finalize our model, and to compare it with data from an experimental prototype (see figure 3). This will bring us to a discussion where we can compare this device with a bifacial PV-cell without a reflector.

13th International Conference on Concentrator Photovoltaic Systems (CPV-13)
AIP Conf. Proc. 1881, 070004-1–070004-7; doi: 10.1063/1.5001437
Published by AIP Publishing. 978-0-7354-1561-4/$30.00

THE MODEL

The modelling starts by identifying the possible paths of rays, dependent on their initial position and angle. When all ray paths have been identified we focus on the relevant rays, which will be incident on the PV surface. The individual rays will be weighted by the different losses they experience on their path through the model. The angle of incidence and path for a given ray are important in order to calculate the Fresnel, absorption and reflection loss:

- Fresnel loss occurs when light travels through a flat interface between two dielectric media. Generally, the light beam will be divided into a refracted (transmitted) light beam and a reflected light beam without suffering any further losses. The transmission (T) and reflection (R) coefficients are listed below as functions of angle of incidence (θ), the refractive indexes of the first (n_1) and second (n_2) medium, respectively[7]:

$$T\left(\theta,n_1,n_2\right)=\begin{cases}\dfrac{\sin\left(2\theta\right)\sin\left(2\sin^{-1}\left(\dfrac{n_1}{n_2}\sin\left(\theta\right)\right)\right)}{\sin^2\left(\theta+\sin^{-1}\left(\dfrac{n_1}{n_2}\sin\left(\theta\right)\right)\right)\cos^2\left(\theta-\sin^{-1}\left(\dfrac{n_1}{n_2}\sin\left(\theta\right)\right)\right)} & \text{for the TM polarization}\\ \dfrac{\sin\left(2\theta\right)\sin\left(2\sin^{-1}\left(\dfrac{n_1}{n_2}\sin\left(\theta\right)\right)\right)}{\sin^2\left(\theta+\sin^{-1}\left(\dfrac{n_1}{n_2}\sin\left(\theta\right)\right)\right)} & \text{for the TE polarization}\end{cases} \tag{1}$$

$$R\left(\theta,n_1,n_2\right)=\begin{cases}\left[\dfrac{\tan\left(\theta-\sin^{-1}\left(\dfrac{n_1}{n_2}\sin\left(\theta\right)\right)\right)}{\tan\left(\theta+\sin^{-1}\left(\dfrac{n_1}{n_2}\sin\left(\theta\right)\right)\right)}\right]^2 & \text{for the TM polarization}\\ \left[\dfrac{\sin\left(\theta-\sin^{-1}\left(\dfrac{n_1}{n_2}\sin\left(\theta\right)\right)\right)}{\sin\left(\theta+\sin^{-1}\left(\dfrac{n_1}{n_2}\sin\left(\theta\right)\right)\right)}\right]^2 & \text{for the TE polarization}\end{cases} \tag{2}$$

- Material absorption losses are caused by bulk absorption in a material, which the light propagates through. The absorption coefficient γ is the material parameter, while A defines the relative intensity transmitted after a traveled distance in the material of L[7]:

$$A\left(L\right)=\exp\left(-\gamma L\right) \tag{3}$$

- Reflection at metallic surfaces. In principle, the Fresnel equations could describe these losses. However, the refractive index and the significant absorption for metals are often uncertain and difficult to establish. Therefore, the experimentally determined reflection coefficient for a polished metal surface will be used here, instead. We assume that the reflection coefficient is a constant, independent on the wavelength and angle of incidence.

In this case, the PV cell is laminated with a thin glass layer. Therefore, the Fresnel equations are used to determine the loss occurring as light enters the laminate. At first incidence we sum up the power of light transmitted into the glass and assume that all this light will be absorbed by the PV cell. For further pursue of the ray reflected of the glass laminate we also determine the power of the rays reflected after a direct incidence onto the glass laminate,

and can derive a simple angular dependence for their next incidence on the PV surface. In case that, their original incidence is more than 45 deg. relative to the normal of the PV surface they will all hit the PV cell again. Again, we assume that all the transmitted light is absorbed by the PV cell, and now that the second reflection will escape. In Eq.1 and Eq.2 we only consider interfaces, where light enters from air into glass, thus, the refractive indexes, used for air (n_a = 1.00) and glass (n_g = 1.50), can be substituted as $n_a \rightarrow n_1$ and $n_g \rightarrow n_2$.

Material absorption losses occurring when light propagates inside a transparent dielectric material will be neglected (γ = 0) here, because the glass laminate above the PV cells is thin (< 1 mm). However, the reflection coefficients for the metallic surfaces are significant, and here they are set to 95% as it would be for enhanced alumina.

The design, used for the raytracing model, is illustrated in Fig.1(a) for a horizontal cross section. In this design the mirrors are plane surfaces and provide no concentration of the sunlight. The system is a vertical standing bifacial panel, which for simulation purposes is oriented east west. The two reflector plates are connected to the PV cell, and each spans an angle of α = ±45 deg. relative to the bifacial panel. In this work, the reflector only encapsulates half the length of the PV cell. The total length of the illustrated PV cell is 2 L_p.

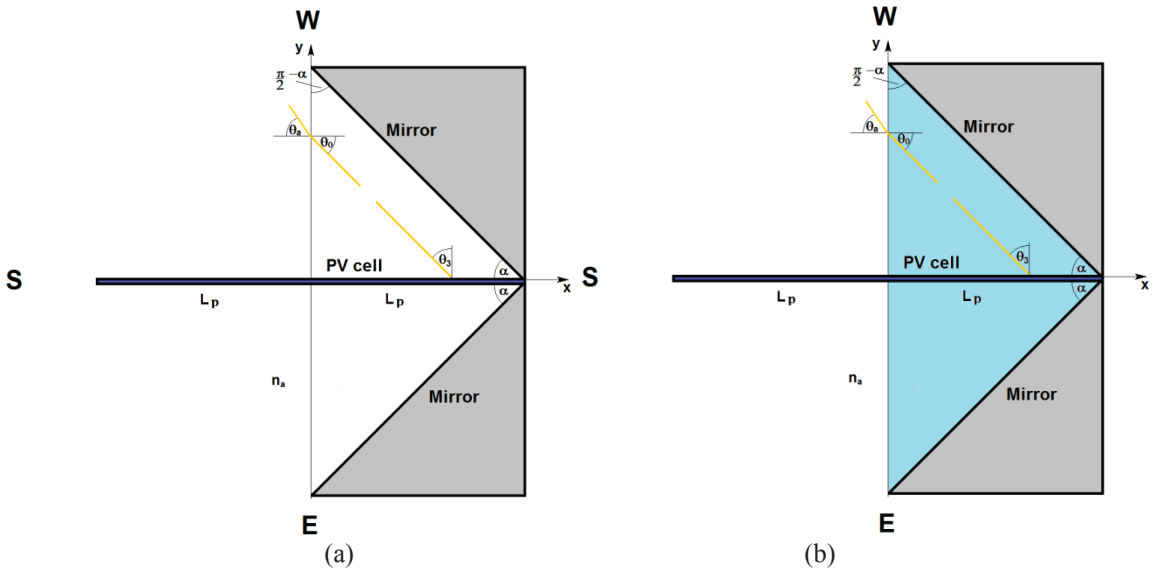

FIGURE 1. (a) Illustration of the current reflector system. (b) Illustration of an earlier reflector system.

Earlier designs (Fig.1(b)) had a bulk material (glass or plastic) inside the reflector, in order to capture light reflected by the reflector in an unfortunate direction, and thus leaving the retroreflector. The capture is achieved by internal reflection or even total internal reflection. However, in this case the volume inside the reflector consists of air only. The extension of the PV cell by the length of L_p away from the retroreflector means that all these escaping light rays are captured directly by the PV cell itself.

Using the model and its assumptions concerning the number of reflections described above, we only need to consider two paths of light entering the retroreflector:

1. Direct incidence onto the PV cell.
2. Reflection in the retroreflector and then incidence onto the PV-cell.

Similarly, the part of the PV cell sticking out from the retroreflector can be handled by two paths as well:

1. Direct incidence onto the PV cell from left.
2. Direct incidence onto the PV cell from the right.

Every time (max. 2) a ray is reflected by a alumina surface we use a reflection coefficient of 95%, as an average value for the reflection coefficient throughout the spectral range of c-Si. The solar elevation (ψ) is determined from the local latitude (φ), the declination of the sun (δ) and the azimuth angle (θ) of the sun relative to the local true south:

$$\psi = \sin^{-1}\left[\sin\varphi\sin\delta + \cos\varphi\cos\delta\cos\theta\right] \tag{4}$$

The schematics of Fig.1 illustrate the models of the vertical retroreflector, and their orientation relative to earth poles. The model combines the ray tracing with solar irradiation data, obtained by a Si-photodetector, which tracks the sun across the sky, and discards the diffuse contribution.

EXPERIMENTS

The solar irradiance is measured with the tracking solar measurement station illustrated in Fig.2. The tracking device maintains at all time normal incidence of the sun light onto the detector. Further, the solar station provides measurements of the diffuse optical contribution onto a horizontal surface (thermopile detector) as well as wind speed and temperature. The solar station is mounted above roof height to ensure no shadowing effects from the surroundings.

FIGURE 2. The tracking solar setup measures the normal incidence of light from the sun. The black sphere obstructs direct sunlight to a horizontal detector, which measures the diffuse light.

The prototype is illustrated in Fig.3. The prototype has a cross section which is very similar to the schematics drawn in Fig.1, see Fig.3(a). The height of the PV cell is 1.8 m, while its width and thickness is 0.16 m and 5 mm, respectively. The height of the reflector and the opening in the cabinet is 2 m in order to avoid shadowing effects near the top and bottom of the PV cell. The prototype is mounted at ground level (Fig.3(b)), and therefore, there will be shadowing effects from the surroundings. Specifically, a tree will provide shadow until midday. The data are obtained for direct comparison with our simulations.

(a) (b)

FIGURE 3. (a) The prototyping setup of the bifacial PV cell with its retroreflector as illustrated in Fig.1. (b) The prototype is mounted on ground level.

The raw data from the systems are sampled with a sample rate of 0.1 S/s. Both, the solar data and the electrical current from the prototype are then low pass filtered with a current averaging algorithm with a flat kernel to an effective sample rate of 0.0042 S/s or approximately 1.0 S/deg. (azimuth angle).

RESULTS

The latitude is set to 55.676° North, which corresponds to the latitude of Copenhagen. The shortest day (21/12), the longest day (23/6) of the year and the day of data acquisition (10/4) are simulated in our model. Preliminary, we assume that the radiance from the sun is constant during its travel across the sky. The simulations are plotted in Fig.4(a) as the normalized irradiances as a function of azimuthal angle (rad.).

As a reference for the simulations we simulate a bifacial panel facing east-west with the same area as PV cell in the retroreflector a well. Figure 4(b) illustrates the simulations for the bifacial panel.

In Table1 the relative integrated power from the individual curves in Fig.4(a) and Fig.4(b) are listed.

TABLE 1. The normalized power obtained in Fig.4 are integrated through a day and listed for the three dates.

System\Seassons	23rd of June	10th of April	21st of Dec.
Bifacial with retroreflector	0.314	0.333	0.230
Bifacial witn no reflector	0.424	0.347	0.102

Clearly, the bifacial PV without a reflector perform best during the summer time when the sun travels through a large azimuth angular interval. However, the bifacial PV cell with the retroreflector perform best during the winter periods where the sun travels through a short angular interval, and with low sun height.

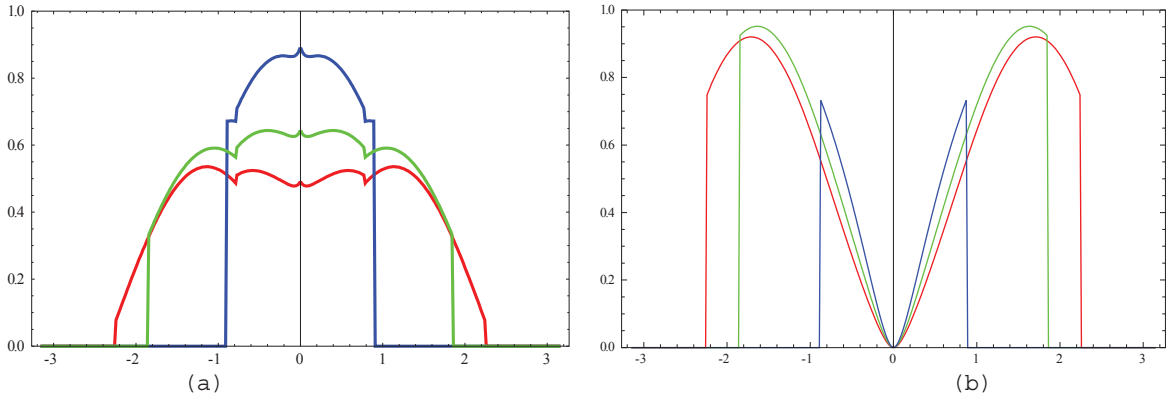

FIGURE 4. The simulations of the bifacial PV cell with the retroreflector (a) and the bifacial PV cell without the reflector (b) plotted versus azimuth angle (rad.). Latitude: 55.676° North, Dates: (red) 23/6, (green) 10/4 and (blue) 21/12.

In Fig.5(a) the direct solar irradiance at normal incidence is plotted as a function of azimuth angle. The data are obtained the 10 of April 2017 near Copenhagen. The sky is not entirely cloud free during the morning. However, during the afternoon we have a reasonably good measurement for comparison with the simulations. Diffuse light is eliminated in this measurement. The diffuse contribution to a detector mounted horizontally is plotted in Fig.5(b).

If we multiply the curve in Fig.5(a) with the simualtion in Fig.4(a) we find the following simulation for the irradiance incident onto the bifacial PV cell with the retroreflector. The result is plotted it in Fig.6(a). In Fig.6(b) the simulated curve in Fig.4(b) of the reference PV is multiplied with the curve in Fig. 5(a) as well. The integrated power from the two systems for the entire day are 56×10^3 and 49×10^3 respectively. The ratio of these two power values indicating that the bare bifacial PV cell collects only 88% of the power collected by the bifacial PV cell with the reflector.

We have not included the diffuse light in the two curves in Fig.5 because, they are not horizontally mounted as the solar detector, which is responsible for this measurement. Secondly, that the two bifacial PV configurations have different opening angles for diffuse light.

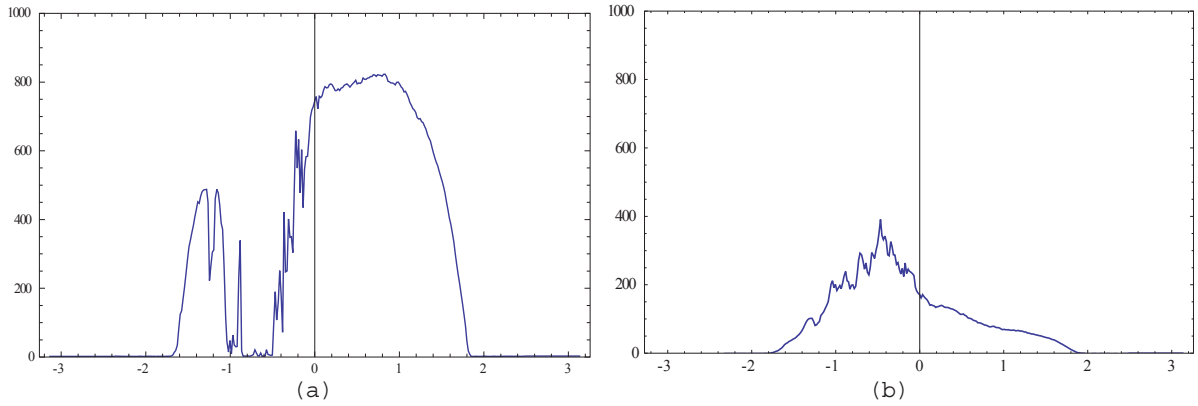

FIGURE 5. Solar data obtained near Copenhagen at the 10th April 2017 are plotted as a function of azimuth angle (rad.). (a) Illustrates the normal incident light from the sun only, while (b) illustrates the diffuse light contribution to a horizontal surface.

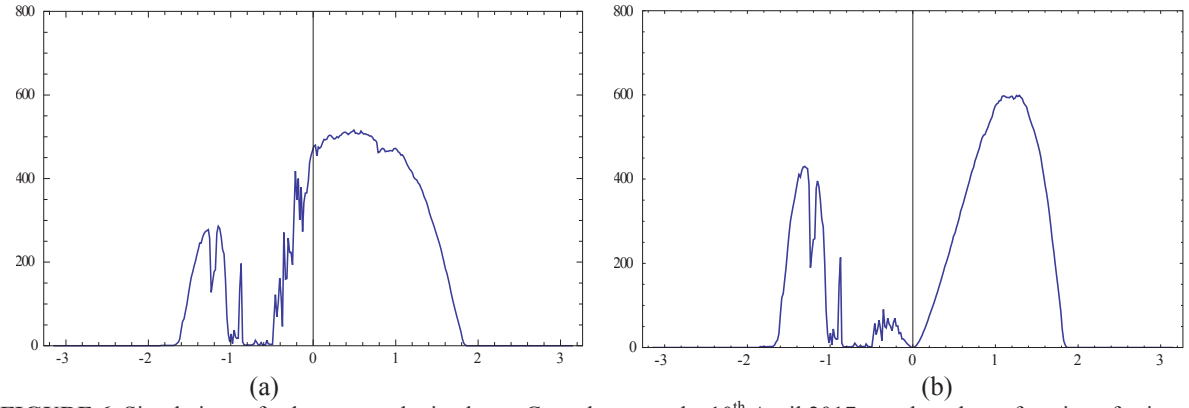

FIGURE 6. Simulations of solar power obtained near Copenhagen at the 10th April 2017 are plotted as a function of azimuth angle (rad.) for the prototype PV (a) and the reference PV (b) with no reflector.

In Fig.7(a) the measurement from the prototyping bifacial PV cell with retroreflector is plotted. These data are acquired simultaneously with the solar data. In Fig.7(b) the simulated curve including the solar light at normal incidence (Fig.5(b)) has been added half the amount of diffuse light as an simple approach to include the diffuse contribution from only half a hemisphere.

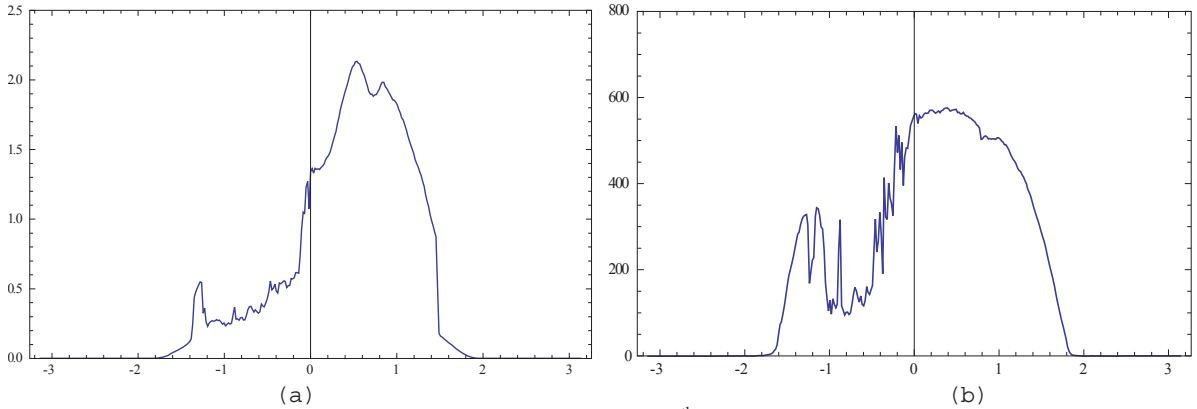

FIGURE 7. (a) Solar data obtained near Copenhagen at the 10th April 2017 by the prototyping bifacial PV cell with retroreflector is plotted as a function of azimuth angle (rad.) (b) The simulated irradiance including solar data for normal incidence and half the measured amount of diffuse light.

DISCUSSION

The results in Table 1 indicates that by integrating the curves in Fig.4 the prototype and the reference PV provides the same total power for the acquisitions obtained at the 10th of April. However, the curves in Fig.6 provide different results for the prototype and the reference PV, which indicates that the reference PV only collects 88% of power collected by the prototype. This is likely to be caused by the attenuation in radiance near sunset, which severely affects the reference PV – compare Fig.4 with Fig.5.

The difference between the measured current produced by the prototype in Fig.7 and the simulated optical irradiance in Fig.6(a) could be caused by several issues. The model includes all rays, which experiences either none or a single reflection. In case of rays reflected of the laminated glass, we still ignore contributions, which are reflected by the reflector before reflection at the laminated glass. Additionally, in case of rays with direct incident on the laminated and at an angle of incidence smaller than 45 deg., few of these might also contribute to the photo current, but are not accounted for in this model.

Of experimental issues we have that the semiconductors do not fill out the PV cell entirely as it is assumed for the simulations. Minor variations in efficiency are expected for the different sub elements in the PV cell. Shadowing effects from trees or buildings have not been included in the model. Specifically, the drop in current, occurring in Fig.5(a) within the range of azimuth angle from -1.2 to -0.5, is caused by clouds on the sky, while the lack of current within the azimuth angular range from -1.6 to -0.2 is caused by the shadowing effect of a nearby three. Therefore, Fig.7(a) and Fig.7(b) should be compared only for the positive angular range. At the moment we do not have a model to including the diffuse light properly in our simulation. However, by simply adding half the measured diffuse irradiation the observed drop in irradiance (Fig.7(b)) in the interval between -0.8 rad. to -0.6 rad. seems reasonable compare with the measured current Fig.7(a).

CONCLUSION AND FUTURE WORK

In this work we have completed our simulation by combining the raytracing model with real solar data. Clearly, the simulations conclude that the reflector can have a strong influence on the application of the PV cell. As Table1 illustrates it, the reflector tested with the prototype here has its clear advantages on a Northern latitude compare to the bare bifacial PV cell. Additionally, we have processed our first power measurement from the prototype and compared them with our simulations.

ACKNOWLEDGMENTS

The project is funded by the Danish Energy Technology Development and Demonstration Programme, project number 64014-0508 “SENSORPOWER – Bifacial PV Energy Reflector Tower”.

REFERENCES

1. G. João, “Testing bifacial PV cells in symmetric and asymmetric concentrating CPC collectors,” *Engineering*, vol. 05, no. 01, pp. 185–190, 2013.
2. A. Moehlecke, F. S. Febras, and I. Zanesco, “Electrical performance analysis of PV modules with bifacial silicon solar cells and white diffuse reflector,” *Sol. Energy*, vol. 96, pp. 253–262, 2013.
3. A. Luque, E. Lorenzo, G. Sala, and S. López-Romero, “Diffusing reflectors for bifacial photovoltaic panels,” *Sol. Cells*, vol. 13, no. 3, pp. 277–292, 1985.
4. R. J. Magasrevy, “Bifacial efficiency at monofacial cost Building Integrated photovoltaic Energy Solutions for the World,” p. 25, 2007.
5. S. Thorsteinsson, M. L. Jakobsen, P. B. Poulsen, P. M. Rødder and K. Rødder, “Vertical reflector for bifacial PV-panels“, part of: IEEE 43rd Photovoltaic Specialist Conference 2016 (ISBN: 9781509027248), pages: 2678-2681, 2016, IEEE.D. L. Davids, “Recovery effects in binary aluminum alloys,” Ph.D. thesis, Harvard University, 1998.
6. M. L. Jakobsen, S. Thorsteinsson, P. B. Poulsen, P. M. Rødder and K. Rødder, “Ray Tracing modelling of a reflector for a vertical bifacial panel“, part of: Proceedings of the 2016 European Photovoltaic Solar Energy Conference and Exhibition 2016, 2016.
7. M. Born and E. Wolf, “*Principles of Optics*” (Pergamon Press, Oxford, 1980).